T-type and N-type Calcium Channels of *Xenopus* Oocytes: Evidence for Specific Interactions with β Subunits

A. E. Lacerda, E. Perez-Reyes, X. Wei, A. Castellano, and A. M. Brown
Department of Molecular Physiology and Biophysics, Baylor College of Medicine, Houston, Texas 77030 USA

ABSTRACT We used amplifying effects of calcium channel beta subunits to identify endogenous calcium channels in *Xenopus* oocytes. Expression of rat brain β_4 increased macroscopic endogenous current magnitude with a small effect on kinetics. In contrast, expression of rat brain/cardiac β_2 produced a much larger increase in current magnitude and dramatically slowed current decay. Low concentrations of ω-conotoxin GVIA irreversibly blocked currents in both uninjected and β_2-injected oocytes. Single channel recordings revealed both T- and N-type calcium channels with conductances of 9 and 18 pS, respectively, in uninjected oocytes and in oocytes expressing either β subunit. Expression of either β subunit slowed average current decay of T-type single channels. Slowing of T-type current decay by expression of β_2 was due to reopening of the channels. N-type single channel average current decay showed little change with expression of β_4, whereas expression of β_2 slowed average current decay.

INTRODUCTION

Voltage-gated calcium channels are multi-subunit membrane proteins that are essential in a wide variety of signal transduction pathways and for coupling of excitation with contraction and secretion (Bean, 1989; Carbone and Swandulla, 1989; Hess, 1990; Tsien and Tsien, 1990). Interactions among calcium channel α_1, α_2-δ, β, and γ subunits are most frequently studied using heterologous expression of the corresponding cRNAs in *Xenopus* oocytes (Nargeot et al., 1992). The α_1 subunit generates Ca^{2+} channel currents, whereas the other subunits modulate the amplitude, voltage dependence, and time course of the currents (Catterall, 1991; Miller, 1992). The use of *Xenopus laevis* oocytes for transient expression of cloned ion channels is widespread (Sigel, 1990). Oocytes express endogenous voltage-gated Na^+, K^+, Ca^{2+}, and Cl^- channels at low and variable levels (Dascal, 1987). Expression of cloned voltage-gated Ca^{2+} channel α_1 subunits alone in *Xenopus* oocytes can produce appropriate currents; however, these currents are often relatively small and must be distinguished from the endogenous voltage-gated Ca^{2+} channel currents present in oocytes. Coexpression of other Ca^{2+} channel subunits, in particular the β subunit, can significantly increase cardiac/brain L-type (Biel et al., 1990; Castellano et al., 1993a; Castellano et al., 1993b; Hullin et al., 1992; Itagaki et al., 1992; Mikami et al., 1989; Perez-Reyes et al., 1992; Singer et al., 1991; Wei et al., 1991; Williams et al., 1992) and brain non-L-type (Ellinor et al., 1993; Mori et al., 1991) α_1 current magnitude. Some brain Ca^{2+} channel α_1 subunit clones produce no discernible currents in *Xenopus* oocytes in the absence of exogenous non-α_1 Ca^{2+} channel subunits (Ellinor et al., 1993; Williams et al., 1992), whereas another clone's current magnitude was unaffected (Soong et al., 1993). The subunit interactions are clouded by observations that exogenous non-α_1 Ca^{2+} channel subunits alter endogenous Ca^{2+} channel currents in *Xenopus* oocytes (Castellano et al., 1993a; Castellano et al., 1993b; Dascal et al., 1992; Singer et al., 1991; Singer-Lahat et al., 1992a; Williams et al., 1992). Moreover, aside from being transient and dihydropyridine-insensitive, the endogenous currents remain a mystery.

To take advantage of the unique opportunity to characterize the effects of cloned β subunits on native oocyte Ca^{2+} channels and to distinguish more clearly endogenous Ca^{2+} channel responses in coexpression experiments, we recorded endogenous currents from uninjected oocytes and oocytes injected with cRNA coding for either rat brain/cardiac β_2 (Perez-Reyes et al., 1992) or rat brain β_4 (Castellano et al., 1993b) subunits. We extended our studies to the single channel level to define biophysically the types of endogenous Ca^{2+} channels present and to provide independent confirmation of our macroscopic recordings free from the technical limitations of two-microelectrode voltage clamp of *Xenopus* oocytes.

MATERIALS AND METHODS

The cloning of full-length cDNAs encoding rat brain β_2 and β_4 has been described previously (Perez-Reyes et al., 1992; Castellano et al., 1993b). In vitro transcription was performed in a volume of 25 μl containing the following: 40 mM Tris-HCl (pH 7.2), 6 mM $MgCl_2$, 10 mM dithiothreitol, 4 mM spermidine, 0.4 mM ribonucleotides, 1 mM $m^7G(5')ppp(5')G$, 0.5 μg of linearized DNA template, and 10 units of T7 RNA polymerase. The mixture was incubated at 37°C for 90 min. After phenol/chloroform extraction and ethanol precipitation, the cRNA product was resuspended in

Received for publication 4 August 1993 and in final form 7 March 1994.

Address reprint requests to Antonio E. Lacerda, Department of Molecular Physiology and Biophysics, Baylor College of Medicine, One Baylor Plaza, Houston, TX 77030. Tel.: 713-798-4700; Fax: 713-798-3475; E-mail: alacerda@mbcr.bcm.tmc.edu.

Dr. Peres-Reyes' present address: Department of Physiology, Loyola University Medical Center, Maywood, IL 60153 USA.

Dr. Castellano's present address: Depto. Fisiología Médica y Biofísica, Universidad de Sevilla, 41009 Sevilla, Spain.

Dr. Wei's present address: Institute of Molecular Medicine and Genetics, Medical College of Georgia, Augusta, GA 30912 USA.

0006-3495/94/06/1833/11 $2.00

0.1 M KCl. cRNA (46 nl of 0.05 mg/ml) was injected into *Xenopus* oocytes using a Drummond Nanoject oocyte injector. Oocytes were maintained in SOS solution (100 mM NaCl, 2 mM KCl, 5 mM HEPES, 1.8 mM $CaCl_2$, 1 mM $MgSO_4$, 2.5 mM pyruvate, and 50 μg/ml gentamicin, pH 7.6) at 19°C on a rotating platform for 4–6 days before testing. Each batch of oocytes was obtained from a new frog. Oocytes were voltage-clamped using a two-microelectrode voltage clamp amplifier (OC-725, Warner Instrument Corp., Hamden, CT). Voltage and current electrodes (1.8–2.4 MΩ tip resistance) were filled with 3 M KCl. The oocytes were impaled in SOS, then the bath solution was exchanged with either of the following (in mM): 5 $Ba(OH)_2$, 90 NaOH, 1 KOH, 0.5 niflumic acid, 0.1 EGTA, and 5 HEPES, adjusted to pH 7.45 with methanesulfonate; or with (in mM): 40 $Ba(OH)_2$, 50 NaOH, 1 KOH, 0.5 niflumic acid, 0.1 EGTA, and 5 HEPES, adjusted to pH 7.45 with methanesulfonate. Experiments were done at 20–22°C. The pClamp system (Axon Instruments, Inc., Foster City, CA) was used for data acquisition.

For single channel recordings, the vitelline membrane was removed manually in a hypertonic solution (Methfessel et al., 1986). Patch pipettes were fabricated from 7052 glass tubing (Garner Glass Co., Claremont, CA), and the tips were coated with Sylgard (Dow Corning Corp., Midland, MI). Single channel currents were recorded with an Axopatch 200A (Axon Instruments). Except for Fig. 3, *Cb* and *Cc* and 4 *B*, data were analog-filtered to 1 kHz (−3 dB) with an 8-pole Bessel filter and digitized at 5 kHz. The patch pipette contained (in mM): 115 $BaCl_2$, 10 HEPES, 1 EGTA, 1 glutathione adjusted to pH 7.4 with *N*-methyl-D-glucamine. The bath composition was (in mM): 140 K-aspartate, 1 $MgCl_2$, 10 EGTA, 10 HEPES adjusted to pH 7.4 with KOH. This solution brought the oocyte resting potential to about 0 mV. Single channel data were idealized with the TRANSIT algorithm (VanDongen, 1992). Maximum likelihood and nonlinear least-squares parameter estimates, likelihood ratio tests, and statistical analyses were performed with TRANSIT and Microsoft Excel Solver and Analysis tools. Critical close times for constructing burst and cluster distributions were chosen to generate an equal number of misclassified intraburst and interburst closed times (Colquhoun and Sakmann, 1985). The number of components in a dwell time distribution was determined by incrementing the number of components until the likelihood ratio test showed no significant increase in likelihood.

Activity of a stretch-sensitive background channel (Methfessel et al., 1986) can be seen in Fig. 4 *A*. In our solution conditions, this channel reverses current direction at 20–30 mV, and its inward unitary current amplitudes are less than T- or N-type Ca^{2+} channels at potentials positive to −30 mV. We assay the presence of this channel by applying voltage steps to 0, 20, and 40 mV. Bi-directional time-independent currents at 0 and 40 mV identify this channel. Ca^{2+} channels are easily distinguished by the presence of inward currents at 20 and 40 mV. All data were obtained at room temperature.

Convolutions were performed in the frequency domain with the Fourier analysis tools in Microsoft Excel. Ideal distributions were used to reduce noise in the convolutions and were generated with maximum likelihood parameter estimates obtained from single channel recordings. Discrete Fourier transforms of first latency probability density functions (pdf) and open, burst, or cluster pdfs were multiplied and the inverse transform of the product calculated to obtain the convolution. For comparison with the results of convolution, ensemble averages were constructed from idealized channel events. For analysis, we chose data obtained at 20 mV to minimize any effect of stretch-activated channels. Under our recording conditions, 20 mV is close to the reversal potential of these channels.

All single channel data presented in Table 1 were obtained from cell-attached patches with 115 mM Ba^{2+} solution in the patch pipette and 140 K-aspartate solution in the bath. Burst duration and cluster duration values shown in Table 1 are from the slowest component of maximum likelihood parameter estimates. First latency values for Table 1 only were obtained from nonlinear least-squares fits to cumulative first latency probabilities. The number of components in multiexponential pdfs was determined with the maximum likelihood ratio test (see above).

TABLE 1 Comparison of T-type (9 pS) single channel properties in uninjected and β_2-injected oocytes at 20 mV

Parameter	Uninjected	β_2-injected
Openings per burst	1.68 ± 0.12 (n = 5)	2.19 ± 0.34 (n = 4)
Burst duration (ms)	3.57 ± 0.68 (n = 5)	10.29 ± 2.84 (n = 4)
Cluster duration (ms)	30.16 ± 4.64 (n = 4)	76.92 ± 34.87 (n = 4)
Ensemble peak p_o	43.28 ± 8.75 (n = 5)	62.13 ± 10.49 (n = 4)
Ensemble mean p_o	9.16 ± 2.20 (n = 5)	42.43 ± 7.50 (n = 4)*
Fraction of nulls	0.15 ± 0.02 (n = 5)	0.09 ± 0.03 (n = 4)
Openings per record	13.02 ± 2.93 (n = 5)	59.61 ± 11.55 (n = 4)*
Ensemble τ_m §	1.00 ± 0.25 (n = 5)	3.14 ± 0.36 (n = 4)‡
Ensemble τ_h §	52.9 ± 18.5 (n = 5)	615.3 ± 221.7 (n = 4)¶
Steady state I_{ss} §	2.37 ± 0.89 (n = 5)	19.62 ± 5.11 (n = 4)*
First latency fast τ	3.62 ± 1.02 (n = 5)	4.06 ± 0.98 (n = 4)
First latency slow τ	74.0 ± 21.3 (n = 4)	57.2 ± 21.7 (n = 4)
Open time fast τ	0.92 ± 0.25 (n = 5)	1.07 ± 0.27 (n = 4)
Open time slow τ	7.08 ± 3.89 (n = 2)	3.59 ± 0.70 (n = 4)
Closed time τ_1	1.10 ± 0.14 (n = 5)	0.69 ± 0.19 (n = 3)
Closed time τ_2	5.96 ± 1.14 (n = 5)	3.33 ± 1.08 (n = 3)
Closed time τ_3	97.64 ± 10.03 (n = 5)	31.39 ± 2.92 (n = 3)‡

Values are displayed as mean ± SEM of mean (n = number of observations).

*‡ Two-sample Student's t-test assuming unequal variance. Values of p obtained from two-tailed test. * Values of $p \leq 0.05$; ‡ $p \leq 0.01$.

§ Parameters from nonlinear least-squares fit to $I(t) = \text{amp} \cdot (1 - \exp(-t/\tau_m)^2 \cdot \exp(-t/\tau_h) + I_{ss}$.

¶ $p = 0.016$ for a two-tailed test using the Wilcoxon two-sample statistic, a nonparametric statistic.

RESULTS

Macroscopic currents and pharmacology

Endogenous Ca^{2+} currents recorded with the two-microelectrode voltage clamp technique were detectable (>5 nA with 40 mM Ba^{2+} as charge carrier) in 61% (11/18) of the batches of uninjected oocytes that were tested. The batches that express endogenous currents can be subclassified further (Dascal et al., 1992) into "native" (5 to 20 nA, 5/18 batches) and "variant" (>20 nA, 6/18 batches).

Injection of cRNAs for either rat brain β_2 (Perez-Reyes et al., 1992) or β_4 (Castellano et al., 1993b) subunits increased the magnitude of endogenous currents (Fig. 1 *A*). Normalization of the currents to the maximum observed (Fig. 1 *B*) demonstrates that this stimulation by the β subunits occurred without a change in the activation threshold. In contrast, we have shown previously that β subunits shift the activation threshold of the cardiac L-type α_1 (CaCh2a) subunit (Wei et al., 1991; Perez-Reyes et al., 1992; Castellano et al., 1993a, b). β_2 had the largest effect on peak currents (11-fold stimulation at 0 mV test potentials) and had a profound effect on the inactivation rate (Fig. 1, *C* and *D*). In fact, β_2-stimulated currents showed no inactivation during 400 ms test pulses to 0 mV. However, inactivation could be observed at more positive test potentials (Fig. 1 *D*). Inactivation of β_4-stimulated currents was slightly slower in comparison with currents from uninjected oocytes (Fig. 1 *D*).

Endogenous macroscopic currents from uninjected oocytes were irreversibly blocked (68%, n = 2) by ω-conotoxin-GVIA (ω-CgTx) at 0.3 μM with 5 mM Ba^{2+} as the charge carrier in "variant" oocytes (data not shown) and approximately 50% by ω-aga-IIIA spider venom at 0.2 μM in randomly selected oocytes (J. D. Mills, A. Kondo, E. Perez-Reyes, and M. E. Adams, unpublished data). We used

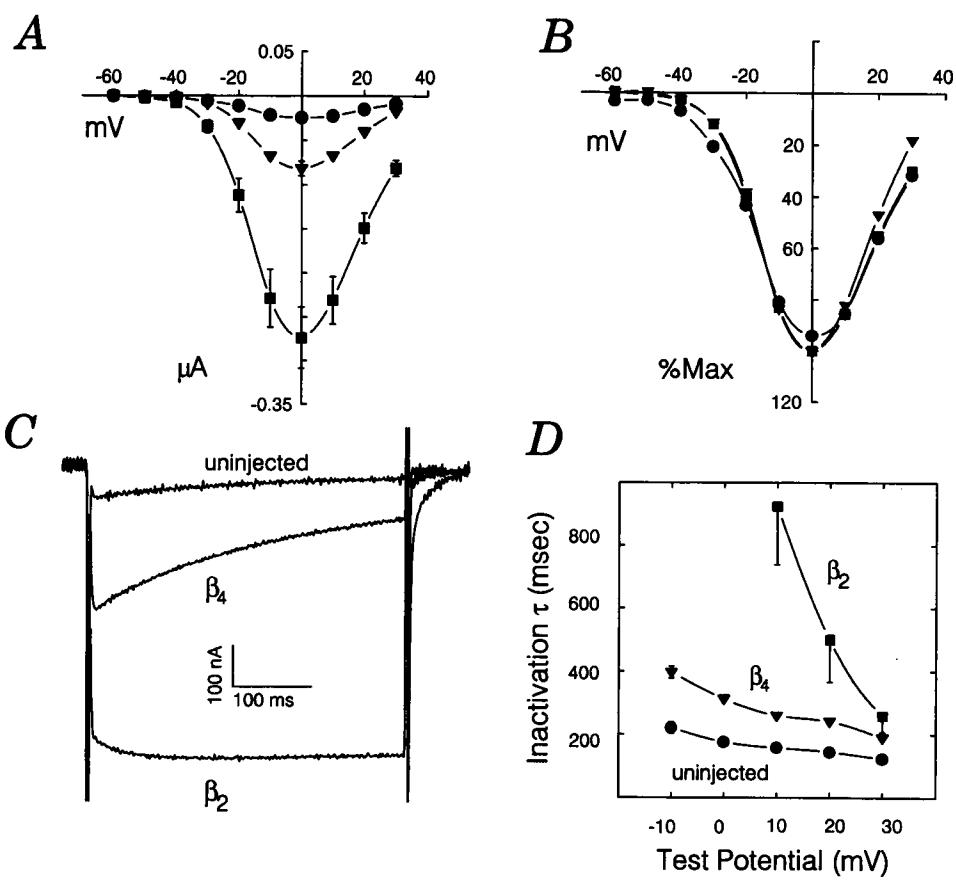

FIGURE 1 Expression of β_2 alters the decay of endogenous *Xenopus laevis* oocyte Ca^{2+} channel currents. (*A*) Mean peak Ca^{2+} channel current (±SEM) is plotted as a function of test potential: uninjected (●), $n = 16$; β_4-injected (▼), $n = 19$; or β_2-injected (■), $n = 6$. The charge carrier was 5 mM Ba^{2+}. The holding potential was −80 mV. (*B*) The currents from each oocyte shown in *A* were normalized to the peak current observed ($100 \times I_{test}/I_{max}$), averaged, then plotted (mean ± SEM) as a function of test potential. (*C*) Three current traces obtained after test pulses to +20 from −80 mV from uninjected, β_2-, and β_4-injected oocytes are superimposed. The charge carrier was 40 mM Ba^{2+}. The data were filtered at 200 Hz and digitized at 1000 Hz. Linear background and capacitive transient currents were subtracted using a P/4 prepulse routine. Residual capacitive current transients due to saturation of the data recording system are truncated. (*D*) Mean (±SEM) inactivation τ is plotted as a function of test potential. Same symbols and n as in *A*. Currents obtained during 400 ms test pulses were fit with two exponentials using pClamp software. Data in *A*, *B*, and *D* were obtained with 5 mM Ba^{2+} and in *C* with 40 mM Ba^{2+} solutions in the bath.

β_2-stimulated currents to characterize the ω-CgTx response. Fig. 2 *A* shows the current-voltage relationships obtained from a β_2-injected oocyte before and after addition of 1 μM ω-CgTx. Dose-response analysis (Fig. 2 *B*) indicated that endogenous β_2-injected oocyte channels are inhibited by low doses of ω-CgTx (0.1 μM IC_{50}).

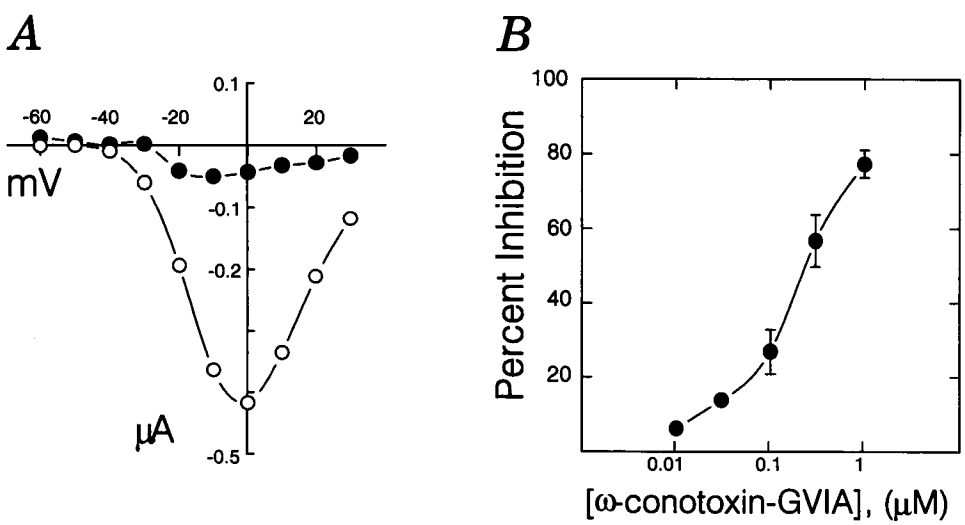

FIGURE 2 ω-conotoxin GVIA inhibition of β_2-induced oocyte Ca^{2+} currents. (*A*) Current-voltage relationships obtained from a β_2-injected oocyte in the absence (○) or presence (●) of 1 μM ω-conotoxin GVIA. (*B*) Cumulative dose response to ω-conotoxin GVIA is plotted as the percent inhibition of control current (measured before toxin addition). The toxin was dissolved in 0.1 mM acetic acid (100 μM), diluted in bath solution, then diluted (10-fold) into the static bath. Currents were measured every 30 s using test pulses to 0 mV. To reduce the contribution of rundown, the response was measured 3–5 min after addition of ω-CgTx. The results shown represent the mean ± SEM from five oocytes obtained from two frogs. All data were obtained with 5 mM Ba^{2+} solution in the bath.

Single channel recordings

For the present single channel study we used two batches of oocytes with large, "variant" endogenous currents and one batch with "normal" endogenous currents. Endogenous voltage-dependent single Ca^{2+} channel currents were recorded in 9, 10, and 5 patches from uninjected oocytes and oocytes injected with β_2 and β_4 cRNA, respectively. In all four patches from uninjected "variant" oocytes, depolarization evoked openings of a large amplitude channel (18 pS; Fig. 3 *Ca*) with very brief open times. Openings of the 18 pS channel from uninjected oocytes were infrequent in pulses to 0 mV, occurred in bursts throughout voltage pulses to 20 mV, and showed a tendency for reduced frequency at the end of pulses to 40 mV ("un"; Fig. 3 *A*).

A second channel type could be distinguished in one of the four patches from "variant" uninjected oocytes and in all five patches from "normal" uninjected oocytes ("un"; Fig. 4 *A*) and had half the amplitude (9 pS; Fig. 3 *Ca*) and longer open times relative to the 18-pS channel. The 18-pS channel was not observed in the five patches from "normal" uninjected oocytes, supporting the identification of these conductances as the result of two classes of independent channels. At all pulse potentials shown in Fig. 4 *A* ("un") voltage-dependent openings of the 9-pS channel from uninjected oocytes occurred in prominent bursts clustered at the beginning of the pulse with few openings after termination of the first burst of openings. The opening frequency of the smaller channel was high at the onset of the voltage pulse to 0 mV (Fig. 4 *Aa*), whereas the larger amplitude channel rarely opened at 0 mV (Figs. 3 *Aa* and 4 *Cc*), indicating that the two channel types have different voltage thresholds. The activation threshold of 0 mV for the 18-pS channel is similar to the threshold for L-type cardiac Ca^{2+} channel α_1 subunits expressed in oocytes under the same solution conditions (A. E. Lacerda, unpublished observations). By analogy with recordings of cloned cardiac L-type Ca^{2+} α_1 subunit single channels measured in the same way, we assign the 18-pS channel to the high threshold class of Ca^{2+} channels and we propose that it is an N-type Ca^{2+} channel.

The 9 pS endogenous channel has a threshold that is 20–30 mV more negative than the high threshold 18 pS endogenous channel and is similar in threshold, kinetics, and conductance to low-threshold T-type channels measured in comparable solution conditions in cardiac myocytes (Nilius et al., 1985) and neurons (Carbone and Lux, 1988; Fox et al., 1987; Nowycky et al., 1985). Values of the time constant for decay of the ensemble average current (τ_h) from uninjected oocytes were consistent with T-type channel kinetics (Table 1). Comparison of data at 0 mV in Figs. 3 and 4 shows that the T-type channel must have a lower voltage threshold for activation. Fig. 4 *Cc* clearly shows the difference in voltage threshold between a patch with a T-type channel and several N-type channels (*Cca*) and a patch with only N-type channels (*Ccb*). The average single channel currents compare favorably with macroscopic currents in the presence of β_2 shown in Fig. 1 *C*. Neither channel is a member of the dihydropyridine-sensitive

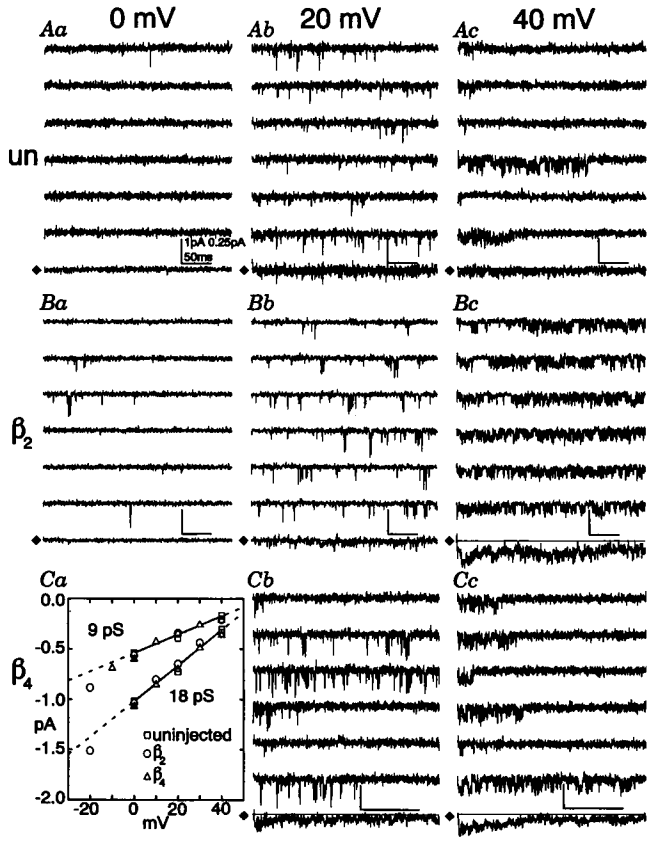

FIGURE 3 N-type Ca^{2+} channel currents in cell-attached patches from *Xenopus* oocytes. Here and in Fig. 4 in each panel of single channel records the horizontal calibration is 50 ms and the vertical calibration is 1 pA for individual records (first 6 traces) and 0.25 pA for the average current (trace 7, below the calibration; marked by ◆). All data were obtained from cell-attached patches with 115 mM Ba^{2+} solution in the patch pipette and 140 mM K-aspartate solution in the bath. Patch potentials for each column of single channel records are indicated across the top and the cRNA injected in each row along the left side of Figs. 3 and 4. Records are consecutive unless otherwise indicated. Smooth horizontal lines through data in selected records indicate the zero current level. From the absence of overlapping N-type openings we infer a single N-type channel was active in the patches shown here (Fig. 3). (*un*) The channels in panel *A* were recorded in a patch from an uninjected oocyte. The patch was held at −120 mV and stepped to the indicated potentials. Records are from six consecutive steps to each potential except trace 6 at 40 mV (*Ac*) and the averages include 15 records at 0 and 20 mV and 19 records at 40 mV. (β_2) In panel *B* channel activity in a patch from an oocyte injected with β_2 cRNA is shown. Averages at 0, 20, and 40 mV were obtained from 33, 21, and 15 records, respectively. (β_4) In panel *C*, *b*, and *c*, channel activity in a patch from an oocyte injected with β_4 cRNA is shown. In this patch no currents were recorded at 0 mV and averages include 28 records at both 20 and 40 mV (data obtained at 10 and 30 mV are not shown). Note the change in time calibration. The data in *Cb* and *Cc* were analog-filtered to 2 kHz (−3 dB) and digitized at 10 kHz. When β_4 cRNA is injected, the decay in the average current at 40 mV (*Cc*) is virtually complete at a time (160 ms) when the β_2 enhanced current is hardly affected (*Bc*). (*Ca*) Unitary *i*–V relations of the T- and N-type channels (9 and 18 pS, respectively). Single channel amplitudes were obtained from Gaussian fits primarily to amplitude histograms of idealized openings or occasionally to all data amplitudes in selected nonidealized records. Each symbol represents the mean of 1–8 data sets from 1–6 patches at each potential. Slope conductance values were obtained by linear regression of pooled data from uninjected (□), β_2- (○), and β_4 (△)-injected oocytes over the voltage range 0–40 mV.

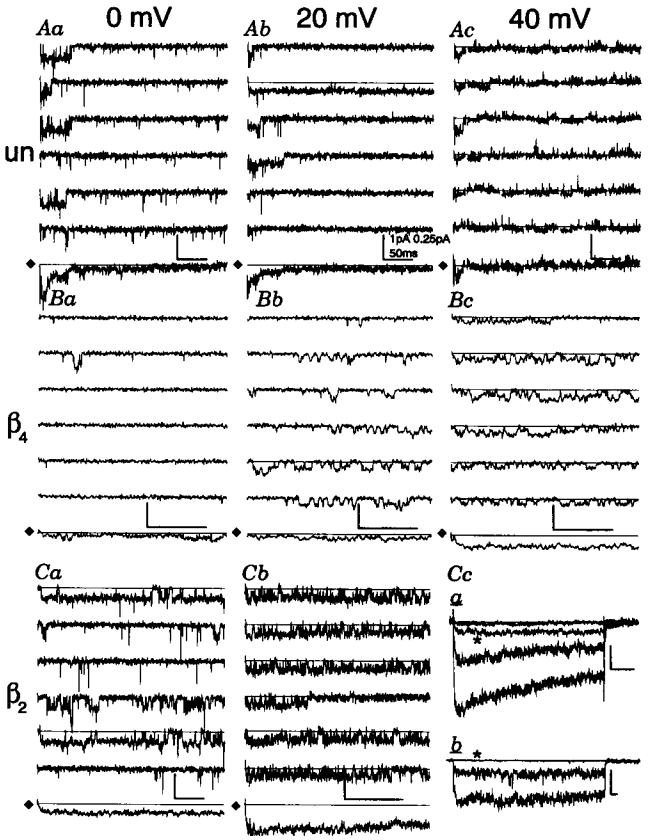

FIGURE 4 T-type Ca^{2+} channel currents in cell-attached patches from *Xenopus* oocytes. The recording conditions were the same as in Fig. 3. Ensemble average records marked by ♦. (*un*) Panel *A* shows channel activity in a patch from an uninjected oocyte. Note the high probability of open state occupancy at the onset of the pulse and its rapid decay. Occasionally a very prolonged opening of the T-type channel was observed, and one such opening is visible in the second record at 20 mV (*Ab*). We estimate two T-type channels were active in this patch from the maximum number of observed simultaneous openings. Activity of a stretch-sensitive background channel can also be seen in *A* (see Materials and Methods). The additional presence of a N-type (18 pS) channel in this patch is confirmed by the large amplitude, brief inward currents at 20 mV. (β_4) Data in panel *B* were filtered at 1 kHz (−3 dB) and digitized at 10 kHz and show channel activity in a patch from a β_4 cRNA-injected oocyte. Note the change in time calibration. This patch appears to have two channels. Note the dramatic change in activation kinetics and the removal of current decay relative to the uninjected oocyte data. Average currents are from 30, 39, and 40 records at 0, 20, and 40 mV, respectively. (β_2) Panel *C*, *a*, and *b* shows T-type channel activity in β_2 cRNA-injected oocytes in two patches. The patch at 0 mV contained at least three N-type channels that obscured the currents of the T-type channel at more positive potentials. Average currents from this patch are also shown in *Cca*. Most notable at 0 mV (*Ca*) is the increased frequency of very prolonged openings seen with expression of the β_2 subunit. T-type channel activity from another patch at 20 mV (*Cb*) recorded at higher bandwidth (2 kHz, −3 dB; note change in time calibration). This patch contained one T-type channel, a stretch channel but no N-type channel. Only data at 20 mV are shown because currents from the stretch channel are not visible at this potential. In *Cca* average currents (76 records at −20 and 79 records at 0, 20, and 40 mV) from the same patch shown in *Ca* stepped to −20, 0, 20, and 40 mV (top to bottom, respectively) from −80 mV are shown superimposed. Average currents from 22 records at each potential of two N-type channels stepped to 0, 20, and 40 mV (top to bottom, respectively) for 1.3 s from −60 mV in another patch are shown superimposed in *Ccb* (note change in time calibration; filter frequency 250 Hz (−3 dB)). An asterisk indicates the average current during the step to 0 mV in both patches.

family of Ca^{2+} channels. Both the 9- and 18-pS channels showed no response to the addition of the dihydropyridine agonist BayK 8644 to the bath.

β_2 and β_4 modulation of N-type 18-pS channel

Unlike the similarity of both β effects on T-type channels (see below), there were differential effects between β_2 and β_4 on N-type channels. β_2 effects on the 18-pS channel were similar to the effects on the 9 pS T-type channel. The ability of β_2 to slow N-type single channel current decay (Figs. 3 *B* and 4 *Ccb*) correlated well with the macroscopic current recordings (Fig. 1 *C*). An interpulse potential of −20 mV was used to inactivate a T-type channel, like those shown in Fig. 4, present in the patch in Fig. 3 *B*. After several minutes, the N-type channel activity also ceased. The N-type channel activity recovered quickly when the interpulse potential was changed to −80 mV. β_4 did not appreciably change the 18 pS N-type single channel kinetics (Fig. 3 *C*).

β_2 and β_4 modulation of T-type 9-pS channel

Injection of exogenous β subunit cRNAs markedly slowed both activation and decay of the 9 pS T-type channel ensemble average currents and increased the number of openings in individual records (Figs. 4, *B* and *C* and 5 *G*; Table 1). For the β_2 subunit, statistically significant effects were found for the number of openings per record, the mean ensemble average probability of opening (p_o), mean ensemble average current and the time constant of the slowest component (τ_3) of the closed time probability density function (pdf). Time constants for activation (τ_m), inactivation (τ_h) and steady-state current estimated from fits of the ensemble average currents to an m^2h Hodgkin-Huxley model (Hille, 1992) were also significantly different. The statistically significant slowing of activation of the ensemble average current by β_2 was not reflected in a significant difference in the latency to first opening (first latencies) of channels from uninjected and β_2 injected oocytes. This apparent discrepancy arises from the indirect contribution of channel first latencies to the time course of ensemble average currents. The ensemble average open probability $p_o(t)$ can be constructed as the convolution of the first latency pdf $f(t)$ with the conditional open probability pdf $m(t)$ (Aldrich et al., 1983). The conditional open probability is defined as the probability of a channel being open at t given that it was open at $t = 0$. The convolution is written as $p_o(t) = f(t) * m(t)$ and can be interpreted as the pdf of the sum of first latencies and conditional open times. The ensemble average current $I(t)$ is obtained from the convolution by the relation $I(t) = N \cdot p_o(t) \cdot i$ in which N is the number of functional channels in the patch and i the unitary current through a single channel at a specified potential.

For uninjected oocytes at 20 mV, convolution of idealized channel first latencies with open times or burst durations (data not shown) failed to overlay $I(t)$ but convolution with cluster durations did (Fig. 5 *A*). Note in Fig. 5, *A* and *B* that

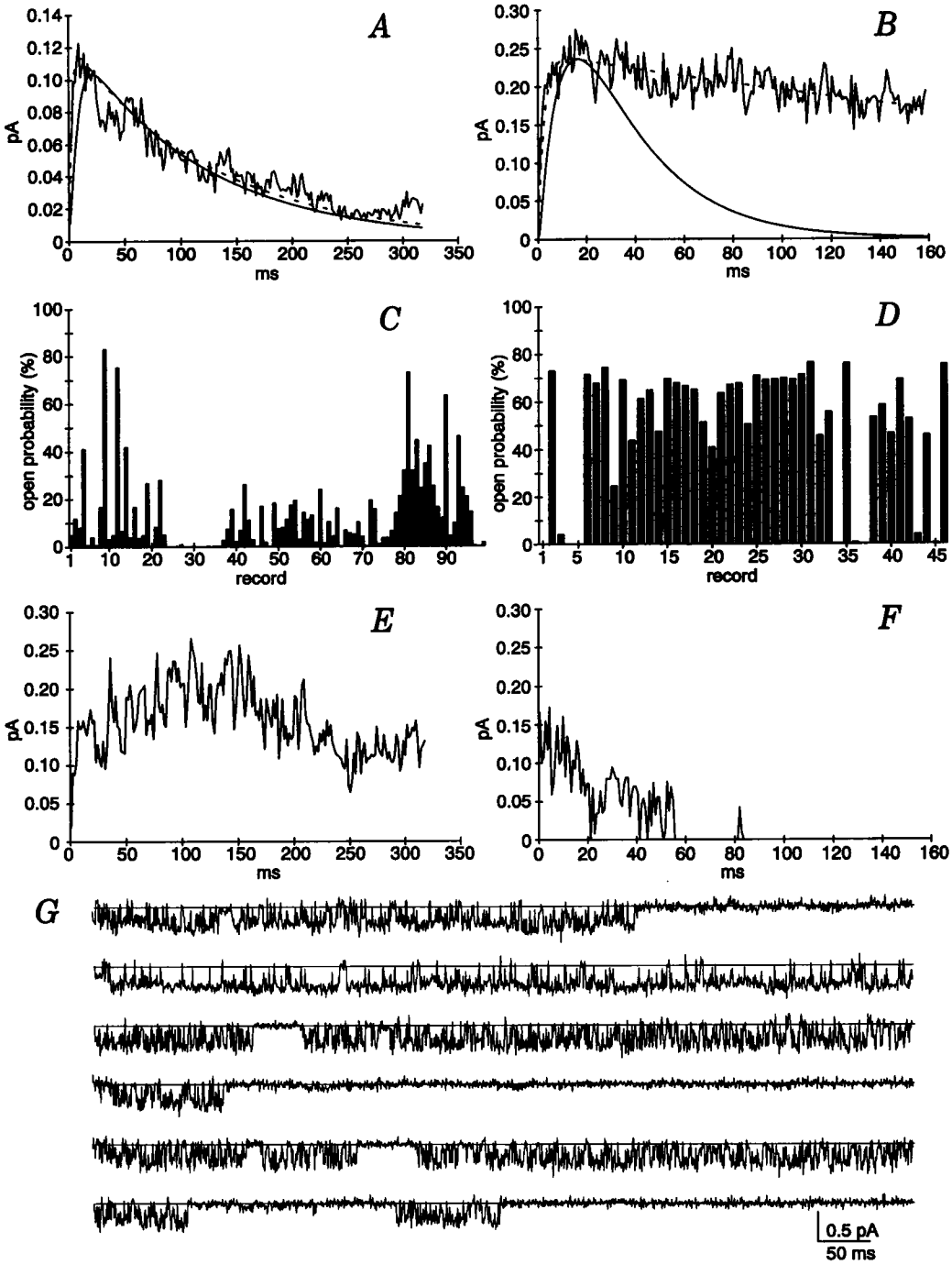

FIGURE 5 β_2 subunit modulation of 9 pS channel kinetics. Convolutions of the first latency pdf with the cluster duration pdf (——) or with the conditional open probability pdf (- - - -) are shown with the ensemble average current of idealized single channels for an uninjected (*A*) and a β_2-injected oocyte (*B*) at 20 mV. Fraction of open state occupancy in each voltage step (record) to 20 mV is shown for the uninjected and the β_2-injected oocytes in panels *C* and *D*, respectively. Ensemble average current (12 records) from steps with open probability $\geq$0.3 from the uninjected oocyte is shown in panel *E*. Ensemble average current (5 records) from steps with open probability $\leq$0.3 from the β_2-injected oocyte is shown in panel *F*. *G*, Consecutive records from a cell attached patch on an oocyte injected with β_2 stepped to 20 mV for 800 ms to show reopening of clusters of bursts. Filter frequency 400 Hz (−3dB). All data obtained from cell attached patches with 115 mM Ba^{2+} solution in the patch pipette and 140 mM K-aspartate solution in the bath.

the convolution of first latency and cluster pdfs rises more slowly than the convolution of first latencies and $m(t)$. For a fixed first latency pdf and a variable decaying exponential pdf, the time to peak of their convolution is proportional to the time constant of the decaying exponential pdf. Slower exponential time constants produce longer times to peak. The significant slowing of activation without significant change in first latency (Table 1) can be explained as the result of a switch of channel kinetics from predominantly single openings and bursts (fast and intermediate duration time con-

stants) to reopening of clusters of bursts (slowest duration time constants) in the presence of β_2. Convolution of first latencies with channel open times and burst durations (data not shown) and cluster durations of β_2-injected oocytes all decayed more rapidly than $I(t)$ (Fig. 5 *B*). The slower decay of ensemble average $I(t)$ is evidence for reopening of the 9-pS channels (Aldrich et al., 1983; Vandenberg and Horn, 1984; Kunze et al., 1986). By inspection of the data in Fig. 5 *G* the reopenings are seen to occur in clusters.

In addition, the 9-pS channel shows heterogeneity in its gating on a record to record time scale. Occasional records show a high probability of opening in uninjected oocytes (Figs. 4 *Ab* and 5 *C*) and conversely occasional records from β_2-injected oocytes (Figs. 4 *Ca* and 5 *D*) show a low probability of opening. The ensemble average of records with high p_o from an uninjected oocyte are shown in Fig. 5 *E*, and similarly records with low p_o from a β_2-injected oocyte are shown in Fig. 5 *F*. Variability in probability of opening from record to record is to be expected, because p_o per record is a random variable. However, the ensemble average of high p_o and low p_o records should differ only by a scale factor if each represents a subset of a random sampling of channel activity from a homogeneous population of identically gating channels. The presence of apparent clustering or runs of records (Fig. 5, *C* and *D*) with similar p_o is further evidence that the channels do not gate identically.

The transient kinetics of the uninjected oocyte ensemble average is present in the average of the low p_o records from the β_2-injected oocyte (Fig. 5 *F*) and similarly, the noninactivating kinetics of the β_2-injected oocyte is reflected in the ensemble average of high p_o records from an uninjected oocyte (Fig. 5 *E*). This suggests that the 9-pS channel has two distinct gating patterns or modes, one comprised of transient channel activity and the other sustained channel activity. Both β_2 and β_4 subunits stabilize the sustained gating mode of the 9-pS channel within the limits of our analysis.

DISCUSSION

Macroscopic currents and pharmacology

Previous reports show that injection of cRNA encoding mammalian Ca^{2+} channel β subunits (in some cases in the additional presence of mammalian α_2-δ) leads to a stimulation of endogenous oocyte Ca^{2+} channels (Singer et al., 1991; Williams et al., 1992; Castellano et al., 1993a, b). We exploited this ability of β subunits to increase endogenous oocyte currents to study the pharmacology and single channel kinetics of these channels. Unexpectedly, we found two endogenous oocyte Ca^{2+} channels in our recordings with distinct kinetics and conductances. A 9-pS channel corresponds most closely in activation threshold, kinetics, and conductance to the class of low threshold, dihydropyridine- and ω-CgTx-insensitive T-type Ca^{2+} channels. The 18-pS channel corresponds most closely in activation threshold, kinetics, and conductance to the high threshold, dihydropyridine-resistant, ω-CgTx-sensitive class of N-type Ca^{2+} channels. A prominent kinetic feature of expression of either β subunit in single channel and macroscopic current recordings is the slowing of endogenous Ca^{2+} channel current decay. The β_2 subunit slowed decay of both the 9- and 18-pS channels, whereas the β_4 subunit slowed decay of the 9-pS channel with little effect on the 18-pS channel. Slowing of endogenous Ca^{2+} current decay kinetics by both β subunits is *opposite* to their accelerating effect on the expressed cardiac L-type α_1 subunit (Perez-Reyes et al., 1992; Castellano et al., 1993a, b). The effect of β_3 on endogenous oocyte currents recorded in our previous work (Castellano et al., 1993a) was similar to the effect of β_4 shown here. Our results indicate that β subunits can have specific interactions with distinct Ca^{2+} channel subtypes and that these interactions can be unique for each β subtype. Of the β subunits we have evaluated, β_2 is the most potent at slowing current decay. Interestingly, β_2 is also the most potent β subunit at slowing decay of a rapidly inactivating, high threshold, Ca^{2+} channel α_1 subunit Doe-1 (Ellinor et al., 1993).

We obtained similar levels of block with ω-CgTx on "variant" uninjected and β_2-stimulated oocyte currents and conclude that exogenous β subunits do not confer ω-CgTx sensitivity to endogenous oocyte channels. Low concentrations of ω-CgTx are specific for N-type Ca^{2+} channels (Feldman et al., 1987; McCleskey et al., 1987; Plummer et al., 1989; but see Swandulla et al., 1991) and block of α_2-$\delta\beta$ cRNA-injected oocyte currents by ω-CgTx has been mentioned (Williams et al., 1992). Block of high threshold Ca^{2+} channels by ω-aga-IIIA is nonspecific (Mintz et al., 1991). For both toxins, a component of endogenous Ca^{2+} current could not be blocked, consistent with the lack of effect of these toxins on T-type Ca^{2+} channels (Feldman et al., 1987; McCleskey et al., 1987; Mintz et al., 1991; see below) or toxin-insensitive channels (Artalejo et al., 1992; Mintz et al., 1992).

Oocytes injected with skeletal muscle mRNAs have provided evidence for two types of endogenous Ca^{2+} channels (Dascal et al., 1992). Several pharmacological, voltage-dependent gating, and kinetic properties of these channels were consistent with those of T- and N-type channels. Ca^{2+} currents in uninjected oocytes were reported to be ω-CgTx (Bourinet et al., 1992; Stea et al., 1993; Umbach and Gundersen, 1987) and crude *Agelenopsis aperta* venom-insensitive (Bourinet et al., 1992). Our results may differ from these previous reports because we selected for study oocytes with large endogenous currents, whereas oocytes used in Umbach and Gundersen (1987) were selected for the absence of currents and, when currents were present, for small currents. Ni^{2+} at 40 μM blocked a transient component present only in uninjected oocytes with large "variant" currents and had no effect on uninjected oocytes with small "native" currents (Dascal et al., 1992), suggesting that oocytes normally express two types of endogenous channels independently. However, Bourinet et al. (1992) found evidence for only one class of endogenous Ca^{2+} channels and observed no dependence of channel pharmacology on current magnitude. Such complex effects seemed more amenable to single channel analysis, and that was our next step.

Single channel recordings

The number of channels uniformly distributed in a β_2-injected oocyte can be estimated from the relation $N = I/(p_o \cdot i)$. The fraction of ω-CgTx-sensitive current was 77% of total peak current in β_2-injected oocytes. For an average peak current of 150 nA at 20 mV, 115 nA is due to N-type channel activity and 35 nA is due to T-type channel activity. Calculating N for the N-type channel with values of 115 nA, 0.5, and 0.8 pA for I, p_o and i, respectively gives 287×10^3 channels per oocyte. Similarly, for the T-type channel with values of 35 nA, 0.5, and 0.3 pA for I, p_o and i, respectively, yields 233×10^3 channels per oocyte. The estimate for the total number of endogenous channels in a typical β_2-injected oocyte is 520×10^3. Using an estimate of oocyte membrane capacitance of 190 nF and assuming a specific capacitance of 1 μF/cm^2 gives a membrane surface area of 19×10^6 μm^2. Average channel density is then $520 \times 10^3/19 \times 10^6 = 0.027$ channels/μm^2. Assuming the membrane in a patch pipette has a free surface area of 2 μm^2 (Sakmann and Neher, 1983), we expect to find 0.054 channels/patch or a channel in 1 of 19 patches. Our best success rate was about 1 channel in 10 patches, which is in fairly close agreement with this model for uniform distribution of channels. We were able to record channels from both the animal and vegetal pole in β_2-injected oocytes. For "normal" oocytes with a peak current of $\leq$20 nA, the expected number of channels per patch is about 10-fold less at 1 channel/200 patches. However, we were able to record currents at a lower success rate of about 1 endogenous channel in 20 patches. Previous work has shown that stretch-activated channels and chloride channels are concentrated at the animal pole of the oocyte (see references in Dascal, 1987). We suspected that the distribution of endogenous Ca^{2+} channels is nonuniform in the uninjected oocytes, and our results support this hypothesis. We were careful to obtain patches from the apex of the animal pole. Patches from the vegetal pole failed to contain endogenous Ca^{2+} channels. Our data suggest that the distribution of endogenous Ca^{2+} channels will become more uniform when exogenous β subunits are expressed.

We have not established directly in single channel recordings the identity of the ω-CgTx-sensitive channel; however, our macroscopic data show that a small toxin resistant component is present, suggesting that only one of the two channels is toxin-sensitive. The channels underlying the toxin-resistant component from "variant" oocytes must be present in smaller quantity or have a smaller conductance or lower p_o relative to the toxin-sensitive component. In single channel recordings from "variant" oocytes, the least frequently observed channel was the 9-pS channel. The 9-pS channel is less abundant in patch recordings from "variant" oocytes, is the only channel we observed in patches from "normal" oocytes, has a low p_o in uninjected oocytes, and a small conductance. The 9-pS channel is most similar in single channel conductance and kinetic properties to the T-type Ca^{2+} channel. We suggest that the 9-pS channel is the source of the toxin-resistant component in macroscopic recordings from "variant" oocytes and is a member of the low threshold, T-type Ca^{2+} channel family. The 18-pS channel is the only other Ca^{2+} channel present in our recordings. Due to the similarity of its single channel conductance and kinetic properties to N-type Ca^{2+} channels, we suggest that the 18-pS channel is the source of the toxin-sensitive component in macroscopic recordings and is a member of the high threshold, ω-CgTx-sensitive N-type Ca^{2+} channel family. The distinctive combinations of single channel conductance, voltage threshold, and average current decay kinetics for each type of endogenous Ca^{2+} channel are consistent with the characteristic combinations of these properties described for T- (Carbone and Lux, 1984; Matteson and Armstrong, 1986; Nowycky et al., 1985) and N-type (Feldman et al., 1987; McCleskey et al., 1987; Nowycky et al., 1985) Ca^{2+} channels (Figs. 3 and 4). From our single channel data, the N-type channel is apparent only in "variant" oocytes. Thus, we propose that the conflicting reports of ω-CgTx sensitivity of endogenous currents are due to variable expression of the 18-pS channel.

Reopening of endogenous calcium channels

Fig. 5 *A* demonstrates that in uninjected oocytes, 9 pS channel activity occurs as single clusters of one or more bursts and the decay of macroscopic current corresponds to the lifetime of these clusters. In comparison, Carbone and Lux (1987) found in dorsal root ganglion neurons, Droogmans and Nilius (1989) in cardiac myocytes and Chen and Hess (1990) in fibroblasts, that convolution of first latencies with burst durations of T-type channels would overlay $I(t)$. Cavalié et al. (1986) showed for cardiac L-type Ca^{2+} channels that convolution of first latencies with cluster durations would overlay $I(t)$. Another distinction is the presence of occasional records from uninjected oocytes in which the channel failed to inactivate, as in Fig. 4 *Ab*. Fig. 5 *B* shows extensive reopening of the 9-pS channel to be the source of the slowly decaying current produced by expression of β_2. Fig. 5 *C–F* also shows that both transient and noninactivating gating modes of the 9-pS channel exist in records from both uninjected and β_2-injected oocytes.

We can model the effects of β subunits on the 9-pS channel assuming β subunits promote channel activity in one of two gating modes that differ by the presence of a transition (ρ) leaving a long-lived closed state. In the transient gating mode, this transition is absent and the transition λ provides access to an absorbing inactivated state (Fig. 6). Because both transient and noninactivating gating modes occur both in the absence and presence of expressed β subunits (Fig. 5), these gating modes are inherent in the 9-pS channel and are not conferred by the β subunit. The channel switches between a gating mode with two closed, an open, and an absorbing inactivated state and another gating mode with three closed states and an open state. The model is focused on possible mechanisms for the effect of β on T-type channel gating and is not intended to provide a detailed description of channel gating kinetics.

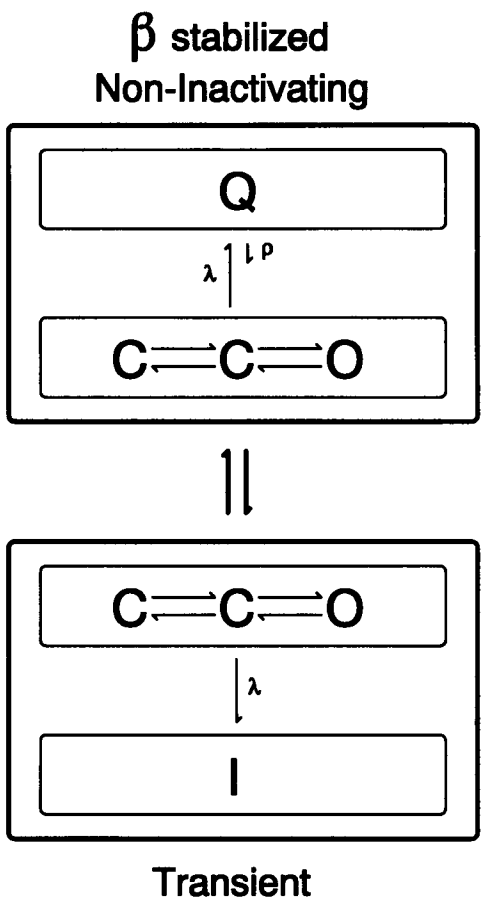

FIGURE 6 Kinetic model of β_2 effect on the 9 pS-channel. The proposed model consists of two gating modes. Each mode consists of two closed states, and one open state. They differ by the presence of an absorbing inactivated state in the transient gating mode and a long-lived close state in the noninactivating gating mode. The β_2 subunit promotes gating in the noninactivating mode. Transitions between modes are voltage-dependent with transient gating favored by positive potentials.

The model makes several predictions about single channel parameters. Clustering of bursts requires three nonabsorbing closed states, so only the noninactivating gating mode can produce clusters of bursts. Mean dwell time in a state is determined by the reciprocal of the sum of transition rates leaving the state. Because λ is the same in both gating modes, its contribution to the dwell times of the short lived open and closed states is the same in each gating mode. The data in Table 1 support this prediction. First latency, burst duration, number of openings in a burst, open time, closed time, and cluster duration are determined by transition rates that are the same in both gating modes. In support of the model, we found no significant difference in these parameters between uninjected and β_2-injected oocytes (Table 1).

However, there is a trend toward an increase in the number of openings in a burst and increased burst and cluster durations. These gating parameters would be expected to increase if β subunits slowed transitions to the inactivated state rather than accelerated transitions out of a long-lived closed state. The fact that a trend is observable in burst gating parameters and the observation of a significant decrease in the time constant of the slowest component of the closed time distribution (τ_3, Table 1) is evidence for β subunit-specific effects on transitions within a gating mode. We propose that β subunits can affect α_1 gating at two levels. At one level, effects that are common to all β subunit isoforms occur by stabilizing particular gating modes intrinsic to each α_1 subunit. At a second level, β subunit isoform-specific effects occur by altering transitions within particular α_1 subunit gating modes. In this view, the primary effect of β_2 and β_4 on the 9-pS channel is to stabilize the intrinsic noninactivating gating mode of this channel in a β subunit isoform-independent way. In support of this, β_2 and β_4 appear equivalent in their ability to promote the noninactivating gating mode of the 9-pS channel (Fig. 4, *B* and *C*). We expect that transitions between the gating modes are voltage-dependent, with the transient mode preferred at stronger depolarization because the effect of β_2 is greatest at low voltages and is reduced at stronger depolarizations (Fig. 1 *D*).

A remarkable feature in Table 1 is the lack of a significant effect of the β_2 subunit on the peak or maximal ensemble average $p_o(t)$. For the 9-pS channel, a substantial increase in peak macroscopic current magnitude can not be due to an increase in the peak $p_o(t)$ of the channel. Because the peak $p_o(t)$ is already about 50%, the maximal increase possible is twofold. Larger increases require effects of β_2 on channel assembly, stability, or transport to the surface membrane (Brust et al., 1993).

Although the slowing of ensemble average current decay by β_4 of the 9-pS channel is similar to the dramatic effect of β_2, the effect of β_4 on macroscopic current recordings is manifested primarily as an increase in peak current (Fig. 1, *A* and *C*) with a small slowing of macroscopic current decay during a pulse (Fig. 1 *D*). Expression of β_4 appears to have little effect on the N-type channel. Our estimate of the fraction of total peak current due to N-type channel activity is 77%. This estimate is based on the data in Fig. 2 *B* in which 1 μM ω-CgTx blocked 77% of peak current. The majority of current in β-injected oocytes appears to be due to activity of N-type channels. Because the β_4 subunit has little effect on N-type channel kinetics, we expect that most of the current in β_4-injected oocytes will resemble a scaled version of the current in uninjected oocytes. We expect at most 23% of the current to be noninactivating. Best fit parameter estimates from nonlinear least-squares fits of macroscopic currents like those in Fig. 1 *C* consistently required a steady-state current to fit data from β_4-injected oocytes. The average value at 0 mV was 18% (n = 12), which is in good agreement with our expectation. For comparison, uninjected oocytes gave average values for the steady-state current of 8% (n = 14), and this difference was statistically significant. We suggest that the slowing of the 9-pS channel's kinetics by expression of β_4 is the basis for the slowing of inactivation and the enhanced steady state component observed in β_4 injected oocytes (Fig. 1 *D*). The effect of β_4 may be primarily to facilitate channel assembly (Brust et al., 1993). However, we cannot exclude an effect on the N-type channel kinetics.

Modulation of Ca^{2+} channels by β subunits

Interaction between cloned Ca^{2+} channel subunits and native T-type Ca^{2+} channels has not been previously described. Especially interesting is that the β subunits used here were cloned by homology to the β subunit of the functionally distinct skeletal muscle L-type Ca^{2+} channel. Coexpression of cardiac α_1 and β subunits in our previous work has resulted in subunit-specific acceleration of α_1 current kinetics (Castellano et al., 1993a, b; Perez-Reyes et al., 1992; Wei et al., 1991). Slowing of endogenous oocyte N- and T-type channel kinetics as seen here adds a novel function to the modulatory effects of β subunits. Recently, a brain low voltage-activated, transient Ca^{2+} channel α_1 subunit similar in threshold for activation to T-type Ca^{2+} channels has been cloned and expressed in *Xenopus* oocytes and shown to interact functionally with a brain isoform of the skeletal muscle β_1 subunit (Soong et al., 1993). We note that β subunit modulation of both endogenous N- and T-type channels described here did not result in altered single channel conductance.

Our results suggest that β subunits are important in tailoring spatial and temporal requirements of Ca^{2+} entry for tissue- and cell-specific functions. The observation that brain has the greatest diversity of β subunits and Ca^{2+} current kinetics lends support to this view. For example, in oocytes, the effects of β_2 could produce four different patterns of N- and T-type channel behavior corresponding to native and exogenous β-associated configurations for each type of channel. Differences among β subunit modulatory capacities may account, in part, for the variability in decay rates of N-type channels (Plummer and Hess, 1991; Plummer et al., 1989; Swandulla et al., 1991). We speculate that the sites of interaction between Ca^{2+} channel α_1 and β subunits are strongly conserved because in no case has coexpression failed to modulate current magnitude- and/or voltage-dependent kinetics. Whether the endogenous oocyte Ca^{2+} channels are associated with endogenous β subunits remains to be determined. However, the presence in oocytes of an mRNA homologous to α_2-δ has been described (Singer-Lahat et al., 1992b). Our data also show that native N-type Ca^{2+} channels can be expressed in non-neuronal cells (Durroux et al., 1988; Sher and Clementi, 1991) where they may play a role in development.

The presence in oocytes of T- and N-type Ca^{2+} channels and their modulation by exogenous Ca^{2+} channel β and α_2-δ subunits may explain some of the variability seen in expression and pharmacological characterization of exogenous and endogenous Ca^{2+} channels in *Xenopus* oocytes. Despite this variability, *Xenopus* oocytes proved useful for our purposes; heterologous expression of β subunits established an interaction with T-type Ca^{2+} channels and suggests that these channels belong to the same family as L-, N-, and P-type Ca^{2+} channels (Soong et al., 1993).

We thank Gabrielle Schuster and Wei-Qiang Dong for injection of *Xenopus* oocytes.

This work was supported by grants from the National Institutes of Health: HL-046702 (to E. Peres-Reyes) and HL-37044 (to L. Birnbaumer and A. M. Brown).

REFERENCES

Aldrich, R. W., D. P. Corey, and C. F. Stevens. 1983. A reinterpretation of mammalian sodium channel gating based on single channel recording. *Nature.* 306:436–441.

Artalejo, C. R., R. L. Perlman, and A. P. Fox. 1992. Omega-conotoxin GVIA blocks a Ca^{2+} current in bovine chromaffin cells that is not of the "classic" N type. *Neuron.* 8:85–95.

Bean, B. P. 1989. Classes of calcium channels in vertebrate cells. *Annu. Rev. Physiol.* 51:367–384.

Biel, M., P. Ruth, E. Bosse, R. Hullin, W. Stühmer, V. Flockerzi, and F. Hofmann. 1990. Primary structure and functional expression of a high voltage-activated calcium channel from rabbit lung. *FEBS Lett.* 269:409–412.

Bourinet, E., F. Fournier, J. Nargeot, and P. Charnet. 1992. Endogenous *Xenopus*-oocyte Ca-channels are regulated by protein kinases A and C. *FEBS Lett.* 299:5–9.

Brust, P. F., S. Simerson, A. F. McCue, C. R. Deal, S. Schoonmaker, M. E. Williams, G. Velicelebi, E. C. Johnson, M. M. Harpold, and S. B. Ellis. 1993. Human neuronal voltage-dependent calcium channels: studies on subunit structure and role in channel assembly. *Neuropharmacol.* 32:1089–1102.

Carbone, E., and H. D. Lux. 1984. A low voltage-activated, fully inactivating calcium channel in vertebrate sensory neurons. *Nature.* 310:501–502.

Carbone, E., and H. D. Lux. 1987. Single low-voltage-activated calcium channels in chick and rat sensory neurones. *J. Physiol.* 386:571–601.

Carbone, E., and D. Swandulla. 1989. Neuronal calcium channels: kinetics, blockade and modulation. *Progr. Biophys. Mol. Biol.* 54:31–58.

Castellano, A., X. Wei, L. Birnbaumer, and E. Perez-Reyes. 1993a. Cloning and expression of a third calcium channel beta subunit. *J. Biol. Chem.* 268:3450–3455.

Castellano, A., X. Wei, L. Birnbaumer, and E. Perez-Reyes. 1993b. Cloning and expression of a neuronal calcium channel β subunit. *J. Biol. Chem.* 268:12359–12366.

Catterall, W. A. 1991. Functional subunit structure of voltage-gated calcium channels. *Science.* 253:1499–1500.

Chen, C., and P. Hess. 1990. Mechanism of gating of T-type calcium channels. *J. Gen. Physiol.* 96:603–630.

Colquhoun, D., and B. Sakmann. 1985. Fast events in single channel currents activated by acetylcholine and its analogues at the frog muscle end-plate. *J. Physiol.* 369:501–557.

Dascal, N. 1987. The use of *Xenopus* oocytes for the study of ion channels. *CRC Crit. Rev. Biochem.* 22:317–387.

Dascal, N., I. Lotan, E. Karni, and A. Gigi. 1992. Calcium channel currents in *Xenopus* oocytes injected with rat skeletal muscle RNA. *J. Physiol.* 450:469–490.

Droogmans, G., and B. Nilius. 1989. Kinetic properties of the cardiac T-type calcium channel in the guinea-pig. *J. Physiol.* 419:627–650.

Durroux, T., N. Gallo-Payet, and M. D. Payet. 1988. Three components of the calcium current in cultured glomerulosa cells from rat adrenal gland. *J. Physiol.* 404:713–729.

Ellinor, P. T., J.-F. Zhang, A. D. Randall, M. Zhou, T. L. Schwarz, R. W. Tsien, and W. A. Horne. 1993. Functional expression of a rapidly inactivating neuronal calcium channel. *Nature.* 363:455–458.

Feldman, D. H., B. M. Olivera, and D. Yoshikami. 1987. Omega *Conus geographus* toxin: a peptide that blocks calcium channels. *FEBS Lett.* 214:295–300.

Fox, A. P., M. C. Nowycky, and R. W. Tsien. 1987. Single-channel recordings of three types of calcium channels in chick sensory neurones. *J. Physiol.* 394:173–200.

Hille, B. 1992. Ionic Channels of Excitable Membranes. 2nd Ed. Sinauer Associates, Inc., Sunderland, MA. 607 pp.

Hess, P. 1990. Calcium channels in vertebrate cells. *Annu. Rev. Neurosci.* 13:337–356.

Hullin, R., D. Singer-Lahat, M. Freichel, M. Biel, N. Dascal, F. Hofmann, and V. Flockerzi. 1992. Calcium channel beta subunit heterogeneity:

functional expression of cloned cDNA from heart, aorta and brain. *EMBO J.* 11:885–890.

Itagaki, K., W. J. Koch, I. Bodi, U. Klöckner, D. F. Slish, and A. Schwartz. 1992. Native-type DHP-sensitive calcium channel currents are produced by cloned rat aortic smooth muscle and cardiac alpha 1 subunits expressed in *Xenopus laevis* oocytes and are regulated by alpha 2- and beta-subunits. *FEBS Lett.* 297:221–225.

Kunze, D. L., A. E. Lacerda, D. L. Wilson, and A. M. Brown. 1985. Cardiac Na currents and the inactivating, reopening, and waiting properties of single cardiac Na channels. *J. Gen. Physiol.* 86:691–719.

Matteson, D. R., and C. M. Armstrong. 1986. Properties of two types of calcium channels in clonal pituitary cells. *J. Gen. Physiol.* 87: 161–182.

McCleskey, E. W., A. P. Fox, D. H. Feldman, L. J. Cruz, B. M. Olivera, R. W. Tsien, and D. Yoshikami. 1987. ω-conotoxin: direct and persistent blockade of specific types of calcium channels in neurons but not in muscle. *Proc. Natl. Acad. Sci. USA.* 84:4327–4331.

Methfessel, C., V. Witzemann, T. Takahashi, M. Mishina, S. Numa, and B. Sakmann. 1986. Patch clamp measurements on *Xenopus laevis* oocytes: currents through endogenous channels and implanted acetylcholine receptor and sodium channels. *Pflügers Arch.* 407:577–588.

Mikami, A., K. Imoto, T. Tanabe, T. Niidome, Y. Mori, H. Takeshima, S. Narumiya, and S. Numa. 1989. Primary structure and functional expression of the cardiac dihydropyridine-sensitive calcium channel. *Nature.* 340:230–233.

Miller, R. J. 1992. Voltage-sensitive Ca^{2+} channels. *J. Biol. Chem.* 267: 1403–1406.

Mintz, I. M., V. J. Venema, M. E. Adams, and B. P. Bean. 1991. Inhibition of N- and L-type Ca^{2+} channels by the spider venom toxin omega-Aga-IIIA. *Proc. Natl. Acad. Sci. USA.* 88:6628–6631.

Mintz, I. M., M. E. Adams, and B. P. Bean. 1992. P-type calcium channels in rat central and peripheral neurons. *Neuron.* 9:85–95.

Mori, Y., T. Friedrich, M. S. Kim, A. Mikami, J. Nakai, P. Ruth, E. Bosse, F. Hofmann, V. Flockerzi, T. Furuichi, K. Mikoshiba, K. Imoto, T. Tanabe, and S. Numa. 1991. Primary structure and functional expression from complementary DNA of a brain calcium channel. *Nature.* 350: 398–402.

Nargeot, J., N. Dascal, and H. A. Lester. 1992. Heterologous expression of calcium channels. *J. Membr. Biol.* 126:97–108.

Nilius, B., P. Hess, J. B. Lansman, and R. W. Tsien. 1985. A novel type of cardiac calcium channel in ventricular cells. *Nature.* 316: 443–446.

Nowycky, M. C., A. P. Fox, and R. W. Tsien. 1985. Three types of neuronal calcium channels with different calcium agonist sensitivity. *Nature.* 316: 440–443.

Perez-Reyes, E., A. Castellano, H. S. Kim, P. Bertrand, E. Baggstrom, A. E. Lacerda, X. Y. Wei, and L. Birnbaumer. 1992. Cloning and expression of a cardiac/brain beta subunit of the L-type calcium channel. *J. Biol. Chem.* 267:1792–1797.

Plummer, M. R., D. E. Logothetis, and P. Hess. 1989. Elementary properties and pharmacological sensitivities of calcium channels in mammalian peripheral neurons. *Neuron.* 2:1453–1463.

Plummer, M. R., and P. Hess. 1991. Reversible uncoupling of inactivation in N-type calcium channels. *Nature.* 351:657–659.

Sakmann, B., and E. Neher. 1983. Geometric parameters of pipettes and membrane patches. *In* Single-Channel Recording. B. Sakmann and E. Neher, editors. Plenum Press, New York. 37–51.

Sher, E., and F. Clementi. 1991. Omega-conotoxin-sensitive voltage-operated calcium channels in vertebrate cells. *Neuroscience.* 42:301–307.

Sigel, E. 1990. Use of *Xenopus* oocytes for the functional expression of plasma membrane proteins. *J. Membr. Biol.* 117:201–221.

Singer-Lahat, D., E. Gershon, I. Lotan, R. Hullin, M. Biel, V. Flockerzi, F. Hofmann, and N. Dascal. 1992a. Modulation of cardiac Ca^{2+} channels in Xenopus oocytes by protein kinase C. *FEBS Lett.* 306:113–118.

Singer-Lahat, D., I. Lotan, K. Itagaki, A. Schwartz, and N. Dascal. 1992b. Evidence for the existence of RNA of Ca(2+)-channel alpha 2/delta subunit in *Xenopus* oocytes. *Biochim. Biophys. Acta.* 1137:39–44.

Singer, D., M. Biel, I. Lotan, V. Flockerzi, F. Hofmann, and N. Dascal. 1991. The roles of the subunits in the function of the calcium channel. *Science.* 253:1553–1557.

Soong, T. W., A. Stea, C. D. Hodson, S. J. Dubel, S. R. Vincent, and T. P. Snutch. 1993. Structure and functional expression of a member of the low voltage-activated calcium channel family. *Science.* 260:1133–1136.

Stea, A., S. J. Dubel, M. Pragnell, J. P. Leonard, K. P. Campbell, and T. P. Snutch. 1993. A β-subunit normalizes the electrophysiological properties of a cloned N-type Ca^{2+} channel α_1-subunit. *Neuropharmacol.* 32: 1103–1116.

Swandulla, D., E. Carbone, and H. D. Lux. 1991. Do calcium channel classifications account for neuronal calcium channel diversity? *Trends Neurosci.* 14:46–51.

Tsien, R. W., and R. Y. Tsien. 1990. Calcium channels, stores, and oscillations. *Annu. Rev. Cell Biol.* 6:715–760.

Umbach, J. A., and C. B. Gundersen. 1987. Expression of an ω-conotoxin-sensitive calcium channel in *Xenopus* oocytes injected with mRNA from *Torpedo* electric lobe. *Proc. Natl. Acad. Sci. USA.* 84:5464–5468.

VanDongen, A. M. J. 1992. Transit: a new algorithm for analyzing single ion channel data containing multiple conductance levels. *Biophys. J.* 61: 256*a*. (Abstr.)

Wei, X. Y., E. Perez-Reyes, A. E. Lacerda, G. Schuster, A. M. Brown, and L. Birnbaumer. 1991. Heterologous regulation of the cardiac Ca^{2+} channel alpha 1 subunit by skeletal muscle beta and gamma subunits. Implications for the structure of cardiac L-type Ca^{2+} channels. *J. Biol. Chem.* 266:21943–21947.

Williams, M. E., D. H. Feldman, A. F. McCue, R. Brenner, G. Velicelebi, S. B. Ellis, and M. M. Harpold. 1992. Structure and functional expression of alpha 1, alpha 2, and beta subunits of a novel human neuronal calcium channel subtype. *Neuron.* 8:71–84.